



N-methyl-D-aspartate receptor blockers attenuate bleomycin-induced pulmonary fibrosis by inhibiting endogenous mesenchymal stem cells senescence

Pu Huang^{1,2}, Yan Zhou¹, Xiao-Hong Li³, Yun-Na Zhang¹, Hai-Peng Cheng³, Jia-Feng Fu¹, Wei Liu⁴, Shaojie Yue⁵, Zi-Qiang Luo^{1,6}

¹Department of Physiology, Xiangya School of Medicine, Central South University, Changsha, China; ²Health Management Center, Changsha Central Hospital Affiliated to Nanhua University, Changsha, China; ³Department of Pathology, The Second Xiangya Hospital, Central South University, Changsha, China; ⁴Xiangya Nursing School, Central South University, Changsha, China; ⁵Department of Pediatrics, Xiangya Hospital, Central South University, Changsha, China; ⁶Hunan Key Laboratory of Organ Fibrosis, Central South University, Changsha, China

Contributions: (I) Conception and design: All authors; (II) Administrative support: ZQ Luo; (III) Provision of study materials or patients: ZQ Luo, S Yue; (IV) Collection and assembly of data: P Huang; (V) Data analysis and interpretation: P Huang; (VI) Manuscript writing: All authors; (VII) Final approval of manuscript: All authors.

Correspondence to: Zi-Qiang Luo. Department of Physiology, Xiangya School of Medicine, Central South University, 110 Xiangya Road, Changsha 410078, China; Hunan Key Laboratory of Organ Fibrosis, Central South University, 110 Xiangya Road, Changsha 410078, China. Email: luoziqiang@csu.edu.cn.

Background: A large number of our previous studies showed that endogenous glutamate and N-methyl-D-aspartate receptor (NMDAR) activation may be involved in various types of acute lung injury, airway inflammation, asthma, and pulmonary fibrosis. In animal models, the transplantation of exogenous bone marrow mesenchymal stem cells (BM-MSCs) is the most promising treatment for idiopathic pulmonary fibrosis. However, there are limited reports on the status of endogenous BM-MSCs in the process of bleomycin-induced pulmonary fibrosis in animals.

Methods: We constructed a mouse model of bleomycin-induced pulmonary fibrosis. *In vitro*, the senescence model of BM-MSCs was constructed with hydrogen peroxide and high concentration of N-methyl-D-aspartate (NMDA). The changes in aging-related indexes were detected by senescence associated beta-galactosidase (SA- β -gal) staining, western blot, flow cytometry and real time-PCR. The epithelial-mesenchymal transformation (EMT) changes of mouse lung epithelial cells (MLE-12) co-cultured with senescent BM-MSCs were detected by immunofluorescence and western blotting.

Results: We observed that endogenous BM-MSCs senescence occurs during bleomycin-induced pulmonary fibrosis in mice, and the model group had a higher expression level of the NMDAR subunit than the control group. We observed a significant increase in NMDAR subunit expression in a hydrogen peroxide-induced senescent cell model *in vitro*. BM-MSCs showed senescence-related phenotype and cell cycle arrest after high concentration of NMDA treatment. At the same time, the expression levels of the classic Wntless and int-1 (Wnt) pathway protein β -catenin and downstream cyclin D1 also changed. In the co-culture of aged BM-MSCs and MLE-12 cells, EMT can be promoted in MLE-12 cells, and MK-801 can partially antagonize the occurrence of EMT. The NMDAR antagonist can partially prevent the above phenomenon.

Conclusions: High concentrations of NMDA can promote senescence of BM-MSCs. NMDAR blockers may inhibit endogenous BM-MSCs aging through the WNT signaling pathway, thereby reducing the effect of bleomycin-induced pulmonary fibrosis.

Keywords: Bone marrow mesenchymal stem cells (BM-MSCs); idiopathic pulmonary fibrosis (IPF); N-methyl-D-aspartate receptor (NMDAR); senescence

Submitted Apr 24, 2022. Accepted for publication Jun 06, 2022.

doi: 10.21037/atm-22-2507

View this article at: <https://dx.doi.org/10.21037/atm-22-2507>

Introduction

Idiopathic pulmonary fibrosis (IPF) is a special type of interstitial pneumonia. About 50% of IPF patients develop progressive and irreversible pulmonary scarring within 5 years and finally die of respiratory failure (1). Nidanib and phenidone do not improve survival rates, and thus, lung transplantation remains the only effective treatment (2). In recent years, mesenchymal stem cells, especially bone marrow-derived mesenchymal stem cells (BM-MSCs), have shown potential use in IPF treatment. BM-MSCs can migrate to damaged lung tissues and differentiate into type II alveolar epithelial cells. A variety of growth factors are produced through paracrine action, such as keratinocyte growth factor, hepatocyte growth factor (HGF), and epidermal growth factor (EGF), which can protect the function of epithelial cells, secrete anti-inflammatory cytokines and chemokines, and exert immune regulatory potential to repair and regenerate damaged tissues (3). BM-MSCs have shown good reparative and protective effects after transplantation in animal models of IPF (4-6). As variants of exogenous BM-MSCs transplantation for IPF treatment have been extensively developed and successfully applied in clinical trials (7), researchers have focused on the effect and mechanism of exogenous BM-MSCs transplantation in the treatment of pulmonary fibrosis. However, there are limited reports on the functional status of endogenous BM-MSCs in pulmonary fibrosis.

Animal experiments have demonstrated that the transplantation of exogenous BM-MSCs significantly alleviated IPF (4-6). BM diseases affect lung health and more than 60% of patients receiving BM transplantation experience lung interstitial inflammation (8). Exogenous BM cell transplantation can cure the disease but may exert adverse effects. In general, after tissue injury, stromal cells (9) and hematopoietic precursor cells (10) in the BM migrate to injury sites and become structural cells or fibroblasts. When a fracture occurs, endogenous BM-MSCs can migrate to damaged sites and promote fracture healing (11). These results indicate that endogenous BM-MSCs play an important role in tissue repair. Compared with age-matched controls, BM-MSCs from patients with IPF are defective, exhibiting mitochondrial dysfunction, deoxyribonucleic acid (DNA) damage, and telomere shortening in BM-MSCs.

In addition, BM-MSCs show DNA damage and telomere shortening (12), suggesting that when IPF occurs, the lungs are damaged, and BM cells are altered. However, further studies are needed to confirm this finding.

The N-methyl-D-aspartate receptor (NMDAR) is a glutamate receptor and ion channel that is widely expressed in the central nervous system. The activation of NMDAR subtypes is one of the main causes of glutamate excitatory toxicity, which mediates Ca^{2+} -dependent cell death (13). Glutamate excitatory toxicity mediated by NMDAR activation can lead to neuronal apoptosis, and receptor dysfunction is associated with a variety of neurological diseases (14). NMDAR subunits are expressed in lung and BM-MSCs in addition to the central nervous system (15-17). Abbaszadeh *et al.* (18) found that myocardial cell necrosis and fibrosis were significantly reduced in heart failure rat models pretreated with memantine, an NMDAR inhibitor. We have also published numerous works on NMDAR. Li *et al.* (19) showed that memantine can alleviate lung inflammation in a bleomycin (BLM)-induced acute lung injury mouse model, although further research is needed to determine the role and mechanism of memantine in the prevention and treatment of pulmonary fibrosis. Our previous study showed that BLM-induced IPF mouse BM cells had an increased rate of glutamate release (17). The BM-MSCs of male mice were pretreated with N-methyl-D-aspartate (NMDA) for 24 h and transplanted into BLM-induced IPF female recipient mice. Compared with the normal BM-MSCs transplantation group, BM-MSCs pretreated with NMDA had significantly aggravated IPF, and NMDAR activation eliminated the inhibitory effect of BM-MSCs on (EMT) and fibroblast activation by reducing HGF secretion (17). Moreover, NMDA inhibited the synthesis and secretion of BM-MSCs HGF, and NMDA-pretreated MSC-CM (conditioned medium for MSCs) had no protective effect on BLM-induced MLE-12 cell damage. In addition, NMDAR activation reduces the phosphorylation level of extracellular signal-regulated kinase (ERK)1/2 of BM-MSCs (20). These results suggest that endogenous glutamate release is involved in the progression of acute lung injury and pulmonary fibrosis, and the activation of NMDARs affects the anti-pulmonary fibrosis effect of BM-MSCs.

Our preliminary experiments measured the composition of newborn BM. Fifteen kinds of amino acids were found in the offspring of rats with intrauterine hypoxia, and only glutamate and threonine concentrations were significantly higher than those of normal newborns. In the intrauterine hypoxia group, BM-MSCs proliferation and cell viability decreased markedly. These results suggest that intrauterine hypoxia caused by high concentrations of glutamate may result in excessive activation of important agonist NMDARs and damage the function of BM-MSCs (21). Also, increased glutamate concentration in lung tissue activates NMDARs and mediates the process of acute lung injury and lung fibrosis. In BLM-induced lung fibrosis, glutamate content in the BM is increased, and activated NMDAR impaired the function of BM mesenchymal dryness possibly by reducing HGF secretion (17) and inhibiting the ERK signaling pathway (20).

Along with genome instability, telomere loss, epigenetic change, loss of protein stability, malnutrition, mitochondrial dysfunction, cell aging, stem cell failure, and intercellular communication change (22), cellular senescence is also a sign of aging. It has two major features: permanent cell cycle stagnation and the release of senescence-associated secretory phenotype (SASP) (23). SASP comprises inflammatory cytokines, chemokines, extracellular matrix (ECM) remodeling factors, and growth factors. For instance, interleukin (IL)-6, IL-8, transforming growth factor- β (TGF- β), vascular endothelial growth factor (VEGF), matrix metalloproteinase (MMP), and SASP are involved in multiple biological functions in tumor development and inflammatory response (24). Short-term or acute aging is beneficial to embryonic development (25), wound healing, and tissue repair (26). However, the accumulation and long-term presence of aging cells can become the primary drivers of age-related tissue deterioration and chronic diseases (27). These effects constitute the “double-sided” aspect of cellular senescence. Ionizing radiation or chemotherapeutic drugs induce senescence, which is caused by sustained DNA damage response and induces the expression of the cell cycle inhibitors, p16INK4a and p21 WAF1/CIP1 (28). Despite the growth stagnation and dysfunction of senescent cells, metabolism remains active and continues to create a toxic microenvironment containing multiple SASPs. In addition, a SASP may spread inflammatory factors to neighboring cells, leading to senescent cell accumulation and further tissue dysfunction (24). Normal BM-MSCs can be used for the treatment of IPF and significantly improve fibrosis. However, whether aging BM-MSCs can alleviate fibrotic

lesions is unknown.

We found that the expression of NMDARs on the BM-MSCs of BLM-induced lung fibrosis mice and the intensity of β -galactosidase staining increased significantly. The amino acid content also increased markedly, suggesting that endogenous glutamate secretion increased, which activated NMDARs and thereby mediated the aging process of BM-MSCs. During BLM-induced pulmonary fibrosis in mice, aged BM-MSCs secrete SASP factors, which form a toxic microenvironment locally in the BM, affect surrounding cells, accelerate the accumulation of aged mesenchymal stem cells, and aggravate tissue dysfunction. In lung fibrosis, the secretion of chemokines increases, and some senescent BM-MSCs home to damaged lung tissue and cannot differentiate and replace the necrotic lung epithelial cells because of their impaired differentiation functions. Numerous SASP factors (such as IL-1, IL6, and TGF- β) are secreted, and normal lung epithelial cells undergo EMT through paracrine action, aggravating pulmonary fibrosis. Therefore, this study investigates the changes in aging BM-MSCs, the expression of NMDARs in a BLM-induced lung fibrosis mouse model, whether changes in the aging indicators of BM-MSCs after NMDA treatment specifically activate NMDARs *in vitro*, and whether NMDAR blockers (memantine and MK-801) can alleviate or aggravate this phenomenon. Most of the previous studies tracked the change status of MSCs *in vivo* and observed the outcome of IPF after xenotransplantation of exogenous MSCs. Our study focuses on the status changes of endogenous BM-MSCs during pulmonary fibrosis and the effects of NMDAR antagonists on endogenous BM-MSCs. The possible causes of changes in endogenous BM-MSCs were explored *in vitro*. Many studies of NMDARs have focused on the central nervous system. We not only found that it is expressed on peripheral tissue BM-MSCs, but even mediates the senescence of BM-MSCs, which has not been reported by other studies. We present the following article in accordance with the ARRIVE reporting checklist (available at <https://atm.amegroups.com/article/view/10.21037/atm-22-2507/rc>).

Methods

Source and culture of BM-MSCs

C57BL/6 mouse BM-MSCs (finished cell lines) isolated from mouse BM were purchased from Procell (Wuhan, China, item No. CP-M131). The cells were identified before

leaving the factory, and identification instructions were provided. The complete medium used contained Dulbecco's Modified Eagle Medium/Nutrient Mixture F12 (DMEM/F12) (Gibco, Waltham, MA, USA), 10% fetal bovine serum (FBS, Gibco), 1% glutamine (Solarbio, China), and 1% double antibody (Procell). The cells were cultured in a constant temperature and humidity cell incubator at 37 °C and 5% CO₂ concentration. The BM-MSCs obtained through this method were used for *in vitro* cell experiments.

Primary mouse BM-MSCs were obtained, and C57BL/6 male mice were purchased from Slack (Changsha, China). The models were grouped according to the experimental requirements for 21 days (see the following animal models for the steps), anesthetized, and disinfected. The BM cavities of the long bones of the mice were rinsed with DMEM/F12 complete medium, and the obtained suspension was transferred to a culture flask, which in turn was placed in a constant temperature cell incubator for 48 h. After adherent sub-culturing to the fifth generation, BM-MSCs were identified by flow cytometry for the detection of the following surface antigens: CD29, CD44, CD90, CD31, CD34, and CD45. CD29, CD44, and CD90 were positive, whereas CD31, CD34, and CD45 were negative. BM-MSCs of the fifth generation were used in experiments after identification.

BM-MSc identification and cell cycle flow cytometry

Detection indicators include CD29, CD44, CD90, CD31, CD34, and CD45.

Identification of BM-MSCs

The medium was changed, and digestion was conducted. A single-cell suspension of BM-MSCs was obtained, centrifuged (1,000 rpm for 5 min), and resuspended in phosphate buffer solution (PBS) containing 3% FBS. The cells were counted until the number of cells was about 105. Each cell sample received 2 µL of mouse monoclonal antibodies CD29, CD44, CD90, CD31, CD34, and CD45 (BD, USA) and incubated at 4 °C for 2 h. The cells were washed three times with PBS containing 3% FBS, resuspended, and loaded on a flow cytometer (BD). The expression of each marker on the cells was calculated according to the percentage and mean fluorescence intensity.

Cell cycle

BM-MSCs were digested with 0.25% trypsin pre-warmed at 37 °C for about 1 min, and 5 mL of complete medium was

added to terminate digestion. After centrifugation, the cell pellet was washed with PBS and fixed in pre-chilled 70% ethanol for 30 min on ice. After washing with PBS, the cells were resuspended in PBS containing ribonuclease (Rnase) (200 µg/mL) and incubated at 37 °C for 30 min. Propidium iodide was added to a final concentration of 25 µg/mL, incubated on ice for 30 min, and then analyzed through flow cytometry. Data were statistically analyzed using FlowJo10.0 software (Becton, Dickinson and Company, USA).

Western blot

Detection indicators include N-methyl-D-aspartate-receptor subunit-1 (NMDAR1), N-methyl-D-aspartate-receptor subunit-2A (NMDAR2A), N-methyl-D-aspartate-receptor subunit-2B (NMDAR2B), ki67, human telomerase reverse transcriptase (hTERT), p16, p21, octamer-binding transcription factor 4 (Oct4), Nanog, p-β-catenin, β-catenin, cyclin D1, C-myc, E-cadherin, epithelial cell adhesion molecule (EpCAM), vimentin, and alpha-smooth muscle actin (α-SMA).

BM-MSCs were harvested and lysed with loading buffer [50 mM tris-hydrogen chloride (HCl), pH 6.8; 100 mM dithiothreitol; 4% 2-mercaptoethanol; 2% sodium dodecyl sulfate (SDS); 10% glycerol]. Cell lysates were denatured at a high temperature (95 °C for 10 min) and stored in a -80 °C refrigerator for subsequent use. The lysate was separated via 8–12% (selected according to the molecular weight of different proteins) SDS-polyacrylamide gel electrophoresis and transferred to a polyvinylidene fluoride (PVDF) membrane (pore size 0.22 or 0.45 µm, selected according to the molecular weights of different protein; Thermo Fisher Scientific, Waltham, MA, USA). The membrane was blocked with 5% non-fat milk for 1 h and then incubated with the following antibodies on a shaker overnight at 4 °C: NMDAR1, NMDAR2A, NMDAR2B (Abcam, USA), ki67, hTERT, p16, p21, β-catenin (NOVUS, USA), Oct4, Nanog, p-β-catenin, cyclin D1, C-myc (Proteintech, China), E-cadherin (Affinity, USA), EpCAM, vimentin (Proteintech), and α-SMA (BF9212, Affinity). Blots were then probed with a horseradish peroxidase-conjugated secondary antibody (Santa Cruz Biotechnology), and reactive protein bands were visualized with Western Lightning Plus-ECL (PerkinElmer, Waltham, MA).

Cell counting kit-8 (CCK-8)

A CCK-8 kit (Beyotime, Shanghai, China) was purchased

Table 1 Real-time PCR primer sequences

Name	Organism	Primer sequence (5'-3')
IL6-F	Mice	TAGTCCTTCCTACCCCAATTTCC
IL6-R	Mice	TTGGTCCTTAGCCACTCCTTC
IL-1 β -F	Mice	CTGTGACTCATGGGATGATGATG
IL-1 β -R	Mice	CGGAGCCTGTAGTGCAAGTTG
TGF- β 1-F	Mice	GAGCCCGAAGCGGACTACTA
TGF- β 1-R	Mice	TGGTTTTCTCATAGATGGCGTTG
β -actin-F	Mice	TTCCAGCCTTCCTTCTTG
β -actin-R	Mice	GGAGCCAGAGCAGTAATC

to detect cell viability. Cells were seeded into 96-well plates at a density of 2×10^3 per well. After 24 h, 10 μ L of CCK-8 solution was added to each well and incubated at 37 °C for 3 h. The 96-well plate was placed in a microplate reader (Thermo Scientific, USA), and the optical density (OD) at a wavelength of 450 nm was measured. The medium in each well was replaced with a fresh medium after color development. OD was measured at 0, 24, 48, and 72 h. A curve was drawn according to the OD value, and the results were saved. The experiment was repeated three times for each group.

Quantitative reverse transcription-polymerase chain reaction (qRT-PCR)

An eppendorf (EP) tube and tip (free of RNase enzymes) were used. Total ribonucleic acid (RNA) was extracted from the BM-MSCs or tissues. The quantity and quality of total RNA were assessed using a nanodrop instrument (Thermo Fisher Scientific) and 50–100 ng of RNA was reverse-transcribed from random hexamers with Superscript first strand kit (Invitrogen, Carlsbad, CA, USA). QRT-PCR was performed using a 7900HT qPCR instrument according to the manufacturer's instructions (Applied Biosystems, Foster City, CA, USA). The primer sequences are shown in *Table 1*. The measurement was repeated three times.

Senescence associated beta-galactosidase (SA- β -gal) staining

BM-MSCs were cultured in 12-well plates, washed twice with PBS, and stained using an SA β -gal staining kit (Solebo, Beijing, China) according to the manufacturer's instructions. Dyeing reagents were prepared, and the cells

were incubated with the dyeing reagents at 37 °C without CO₂ for 6 h. The staining results were observed under an inverted microscope (Olympus Japan) and photographed for recording.

BM-MSCs multi-lineage differentiation assay

Passage 5 BM-MSCs were seeded in 12-well plates and incubated with osteogenic induction medium (α -MEM supplemented with 15% FBS, 1% penicillin-streptomycin, 50 mg/L ascorbic acid, 10-8M dexamethasone (Sigma-Aldrich, St. Louis, MO, USA), and 10 mmol/L β -glycerophosphate) for about 2–3 weeks. The cells were then assayed for alkaline phosphatase (ALP). In an adipogenic induction medium (MUBMX-90031 Cyagen, China), kits A and B were alternately cultured for about 3 weeks, and the medium was replaced every 2–3 days. Oil red O staining was then performed, and the staining results were observed with an inverted microscope and photographed for preservation.

ALP staining

An ALP assay kit (Beyotime, China) was used to detect ALP activity. The cells were washed twice with PBS, and then 50 μ L of 0.2% Triton X-100 was added overnight at 4 °C. Approximately 50 μ L of ALP buffer and 50 μ L of matrix solution were added, and the resulting solution was incubated at 37 °C for 15 min. Finally, 100 μ L of ALP chromogenic solution was added.

Oil red O staining

Oil red O (Sigma-Aldrich) staining was performed for the observation of positive cells after adipogenic induction. After fixation with 4% paraformaldehyde for 30 min, cells were gently rinsed with 60% isopropanol and then stained with oil red O dye solution for 30 min at room temperature. The oil red O dye solution was filtered through filter paper before use.

Immunofluorescence staining

The cells were seeded in 6- or 12-well plates, washed three times with PBS, fixed with 2.5% glutaraldehyde, blocked with blocking buffer (Beyotime), mixed with α -SMA (BF9212, Affinity) or E-cadherin (BF0219, Affinity) primary antibodies and fluorescein isothiocyanate (FITC)-labeled

goat anti-rabbit Immunoglobulin G (IgG) as a secondary antibody (1:500), and incubated. The nuclei were stained with 4',6-diamidino-2-phenylindole (DAPI). Fluorescence microscopy (Olympus Japan) photographs were obtained to record the results.

Animal model

Animal experiments were performed under a project license (No. 2019-121) granted by the Ethics Committee of Central South University (Changsha, China) and were performed in accordance with the guidelines of the National Institutes of Health (NIH) for the care and use of animals. A protocol was prepared before the study without registration.

Eighty male C57BL/6 mice were purchased from Slack Jingda Laboratory Animal Company (Changsha, China). The purchased animals were kept in the specific pathogen free (SPF) animal department of Xiangya School of Medicine, Central South University. The animals were randomly divided into groups according to the experimental requirements. Following the administration of sodium pentobarbital, 50 μ L of BLM (2 mg/kg; Kabuskiki Kaisha, Japan) was intraductally injected on the first day. The C57BL/6 mice were then randomly assigned to one of the following groups: (I) control group, intratracheal injection of an equal volume of normal saline; (II) memantine group, intraperitoneal injection of memantine (10 mg/kg/day); (III) BLM group, intratracheal injection of BLM; and (IV) BLM + memantine group, intraperitoneal injection of memantine (10 mg/kg/day) 30 min before BLM injection.

Histopathology

Lung tissue was fixed in 4% paraformaldehyde solution and then embedded in paraffin for the preparation of tissue sections. The sections were visualized for staining after staining with hematoxylin and eosin (HE) and Masson's trichrome. Two researchers analyzed the samples in a double-blind fashion according to the method described by Ashcroft *et al.* (29) to semi-quantitatively determine the severity of fibrosis.

Hydroxyproline assay

Collagen content was detected using a hydroxyproline kit (Nanjing Jiancheng, China) according to the manufacturer's instructions.

Statistical analysis

Experimental data were expressed as mean \pm standard deviation. Differences between groups were determined using one-way analysis of variance and Tukey's test. All statistical analyses were performed using GraphPad Prism software (GraphPad, 6.0 La Jolla, CA, USA). A P value of <0.05 indicated a statistically significant difference.

Results

The NMDAR inhibitor, memantine, can reduce the degree of fibrosis in mice with BLM-induced pulmonary fibrosis

Our previous study found that memantine can attenuate oxidative stress, pulmonary inflammation, and acute lung injury in mice induced by BLM stimulation (19). In the present study, a BLM-induced pulmonary fibrosis model was established, and the treatment time with memantine was extended to 21 days to observe the effect of memantine on pulmonary fibrosis. Mice were randomly divided into four groups: sham operation, memantine, BLM, and BLM + memantine group. The mice received corresponding surgical treatments, and the related indicators were checked. The group that received memantine treatment alone showed no histopathological changes in the lungs compared with the sham-operated group (*Figure 1A,1B*). HE and Masson staining of the lung specimens and assessment of the Ashcroft scores showed that the intratracheal injection of BLM resulted in severe deformation of the lung structure and deposition of collagen fibers in the lungs (*Figure 1A,1B*). Also, hydroxyproline content significantly increased in the BLM group compared with the control group (*Figure 1C*). Memantine treatment partially ameliorated BLM-induced fibrosis (*Figure 1A-1C*). Furthermore, BLM treatment increased the expression levels of α -SMA and vimentin and decreased those of E-cadherin and EpCAM proteins in the lung tissues, whereas memantine treatment partially attenuated BLM-induced changes in these factors (*Figure 1D,1E*).

Memantine can attenuate the senescence of BLM-induced pulmonary fibrosis in mouse BM-MSCs

Mesenchymal stem or stromal cells, which are non-hematopoietic cells, are originally derived from the BM. BM-MSCs are pluripotent stem cells with self-proliferation and multi-directional differentiation potential (30). The isolation and culture of BM-MSCs must

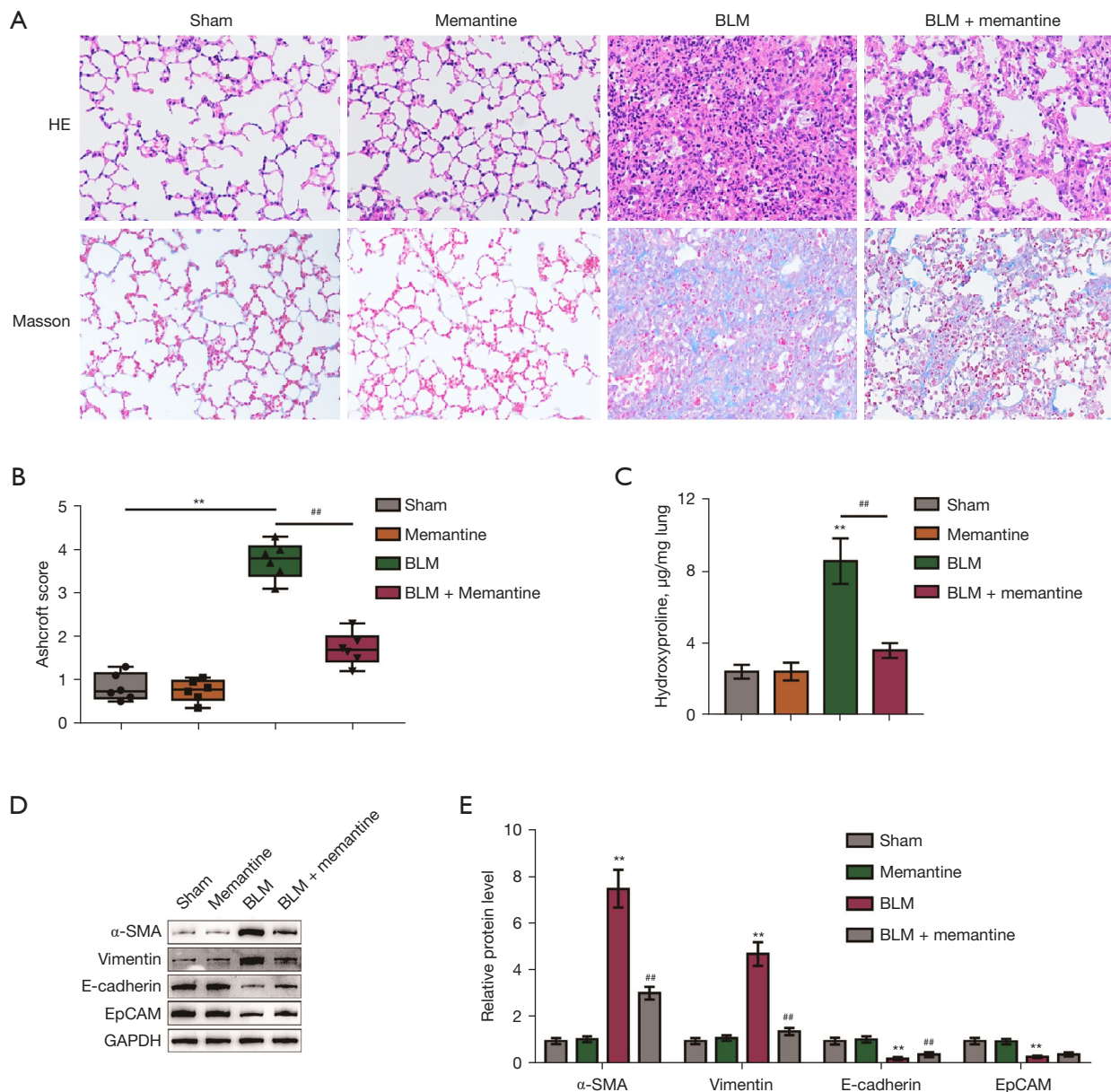


Figure 1 Memantine can reduce the degree of fibrosis in mice with BLM-induced pulmonary fibrosis. (A) HE staining and Masson staining of lung tissue in the sham-operated, memantine, BLM, and BLM + memantine groups ($\times 100$, $n=5$); (B) ashcroft scores of four groups of lung tissue pathological specimens; (C) determination of hydroxyproline content in the four groups of lung tissue samples; (D,E) changes in the protein expression levels of α -SMA, vimentin, E-cadherin, and EpCAM in the four groups of lung tissues. ** $P < 0.01$ vs. Sham; ## $P < 0.01$ vs. BLM ($n=5$). BLM, bleomycin; α -SMA, alpha-smooth muscle actin; EpCAM, epithelial cell adhesion molecule.

meet three criteria (31): (I) when cultured under standard tissue and cell culture conditions, they grow adherently and exhibit a fibroblast-like morphology as well as the ability to undergo clonal proliferation; (II) they can be grown *in vitro*, and differentiate into adipocytes, osteoblasts, and chondrocytes; and (III) they express cell surface marker

molecules, such as CD29, CD73, CD90, and CD105 but not CD45, CD34, CD14, CD11b, CD79a, CD19, or Human Leukocyte class II DR antigens (HLA-DR). Therefore, BM-MSCs isolated from the sham-operated, memantine, BLM, and BLM + memantine groups needed to be phenotyped before use.

The surface markers of BM-MSCs were analyzed by flow cytometry. *Figure 2A* shows the culture morphology of the P0, P2, and P5 generations of primary BM-MSCs. The P5 generation was used in subsequent identification and experiments. The results of flow cytometry analysis (*Figure 2B*) showed that BM-MSCs were CD29 positive (94.46%), CD44 positive (99.36%), CD90 positive (99.61%), CD31 negative (99.84%), CD34 negative (99.96%), and CD45 negative (99.94%).

SA- β -gal staining was then performed. In the BLM group, the positive rate of β -galactosidase staining was significantly higher than those of the other three groups, and memantine partially inhibited the senescence of BM-MSCs (*Figure 2C,2D*). These results suggested that memantine can inhibit the senescence of BM-MSCs.

Increased expression of NMDAR subunits was observed in the BLM-induced pulmonary fibrosis model and senescent cell model

We isolated primary BM-MSCs from the long BM cavity of a BLM-induced pulmonary fibrosis model. This was used for experiments following separation, culture, purification, and identification. The total cell protein was extracted for Western blot (WB) detection, and the expression level of NMDAR1 in the BLM model group was markedly higher than that in the control group (*Figure 3A,3B*). Ionizing radiation or chemotherapeutic drugs may activate induced senescence after sustained DNA damage response and induce the expression of the cell cycle inhibitors, p16 INK4a and p21 WAF1/CIP1 (28). Hydrogen peroxide treatment is a commonly used method of inducing aging. An *in vitro* aging model with hydrogen peroxide was induced in the *in vitro* experiments. Following treatment of the normal BM-MSCs with hydrogen peroxide (100 μ M for 2 h), we found that the positive rate of β -galactosidase staining was notably higher than that of the control group (*Figure 3C*). Moreover, the expression levels of NMDAR1, NMDAR2A, and NMDAR2B in this group were also significantly higher than those in the control group (*Figure 3D,3E*), suggesting that NMDARs may be involved in the mediation of BM-MSCs senescence.

NMDAR activation caused BM-MSCs senescence, and the NMDAR blocker, MK-801, partially ameliorated the senescence of BM-MSCs

NMDA is an agonist that specifically binds to NMDARs,

and MK-801 is a non-competitive NMDAR ion channel antagonist. The NMDAR inhibitor, memantine, is mainly used in animal experiments, while MK-801 is mainly used in *in vitro* cell experiments. β -galactosidase staining is currently recognized as an indicator for detecting cellular senescence. Cell senescence has two major characteristics: (I) permanent arrest of the cell cycle; and (II) release of senescence-related secretory phenotype signaling molecules (SASP factors), such as IL-6, IL-8, TGF- β , VEGF, and MMPs (23,24). In addition, the senescence of BM-MSCs affects multidirectional differentiation, and the expression levels of senescence-related signaling pathway proteins (P53, P21, P16, and Rb) are significantly increased (24,28).

We divided the cells into three groups: PBS, NMDA-treated, and NMDA + MK-801 groups. After each passage, a complete medium containing 3 mM NMDA was used in the NMDA group, while the NMDA + MK-801 group was first pretreated with MK-801 containing 100 μ M for 30 min, and then NMDA was added for the preparation of the final concentration of the medium containing 3 mM NMDA. Next, culturing was performed. NMDA treatment significantly inhibited the cell viability of BM-MSCs (*Figure 4A*), triggered cell cycle arrest in the G1 phase (*Figure 4B*), upregulated the expression of IL-1 β , IL-6, and TGF- β Messenger RNA mRNA (*Figure 4C*) and led to cell senescence (*Figure 4D*). The effects of NMDA on cell viability and cell cycle of BM-MSCs were suppressed by MK-801 was partially attenuated (*Figure 4A,4B*), MK-801 partially downregulated IL-1 β , IL-6, and TGF- β mRNA expression (*Figure 4C*) and MK-801 attenuated the NMDA-induced senescence (*Figure 4D*).

The osteogenic or adipogenic differentiation of the BM-MSCs was induced and determined via ALP and oil red O staining. As shown in *Figure 4E,4F*, NMDA inhibited the osteogenic or adipogenic differentiation potential of the BM-MSCs, and MK-801 partially rescued the differentiation potential. The pluripotency genes, Oct4 and Nanog, are the core components of the regulatory network of genes related to differentiation inhibition. They essentially maintain the pluripotency of stem cells (32) and can directly regulate Deoxyribonucleic acid methyltransferases1 (Dnmt1) to maintain the self-renewal and undifferentiated state of mesenchymal stem cells (33). Human telomerase reverse transcriptase (hTERT) (34) and Ki-67 (35) are classical cell proliferation markers. NMDA treatment, decreased the expression of cell proliferation markers (Ki-67 and hTERT protein), and increased the expression of senescence-related proteins (p16 and p21)

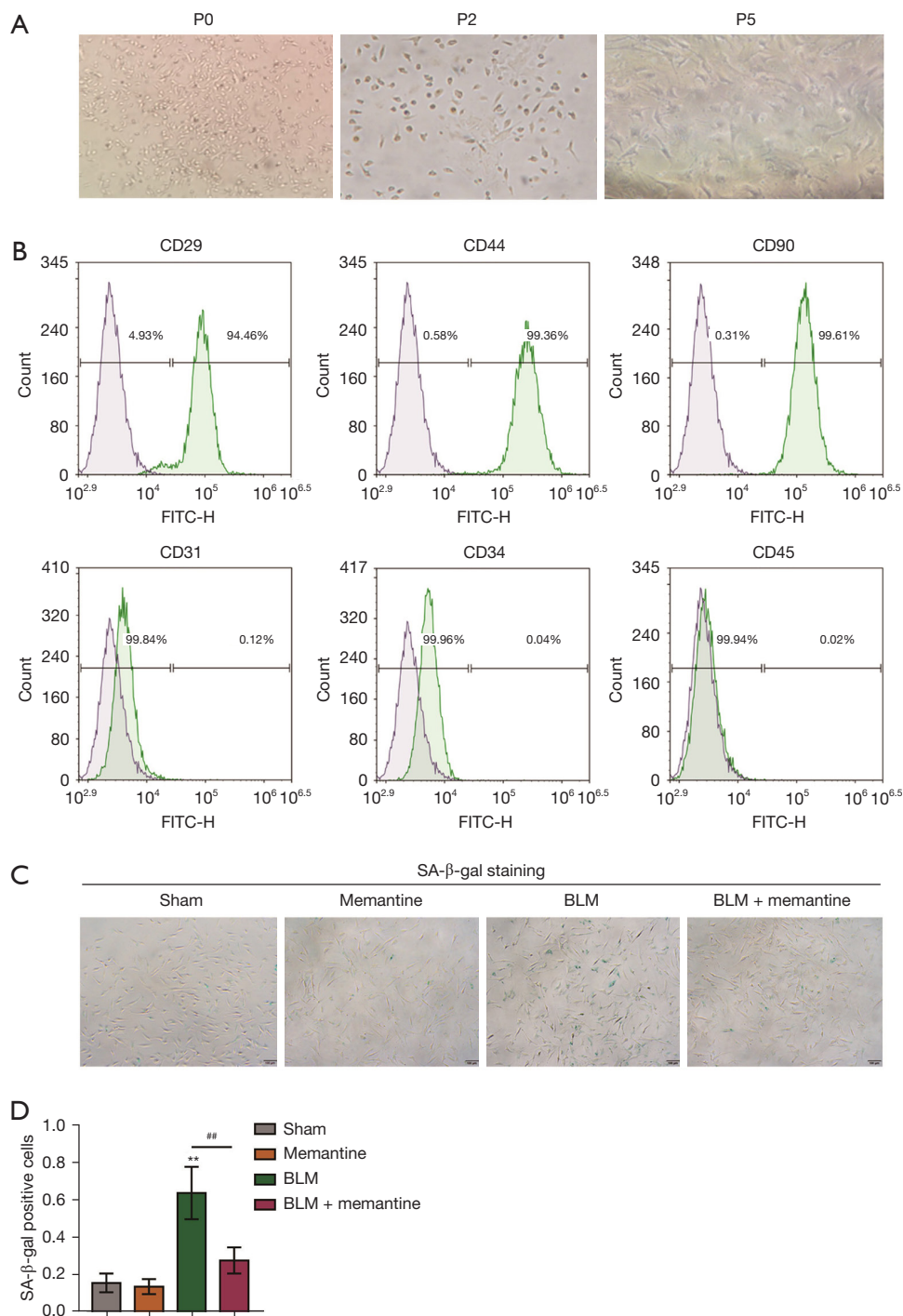


Figure 2 Memantine can attenuate the senescence of BLM-induced pulmonary fibrosis in mouse BM-MSCs. (A) Culture morphology of P0, P2, and P5 generations of the primary BM-MSCs (the picture is displayed at $\times 100$, $n=3$); (B) flow cytometric identification results of primary BM-MSCs, CD29, CD44, CD90 positive cell rate, CD31, CD34, and CD45 negative cell rate ($n=3$); (C,D) β -galactoside of primary BM-MSCs in four groups: sham, memantine, BLM, and BLM + memantine groups. Enzyme staining showed that the BLM model group had the highest positive rate. In the BLM + memantine group, memantine partially inhibited the senescence of BM-MSCs ($\times 40$, $n=3$). $**P<0.01$ vs. sham; $##P<0.01$ vs. BLM. SA- β -gal, senescence associated beta-galactosidase; BLM, bleomycin; BM-MSCs, bone marrow mesenchymal stem cells.

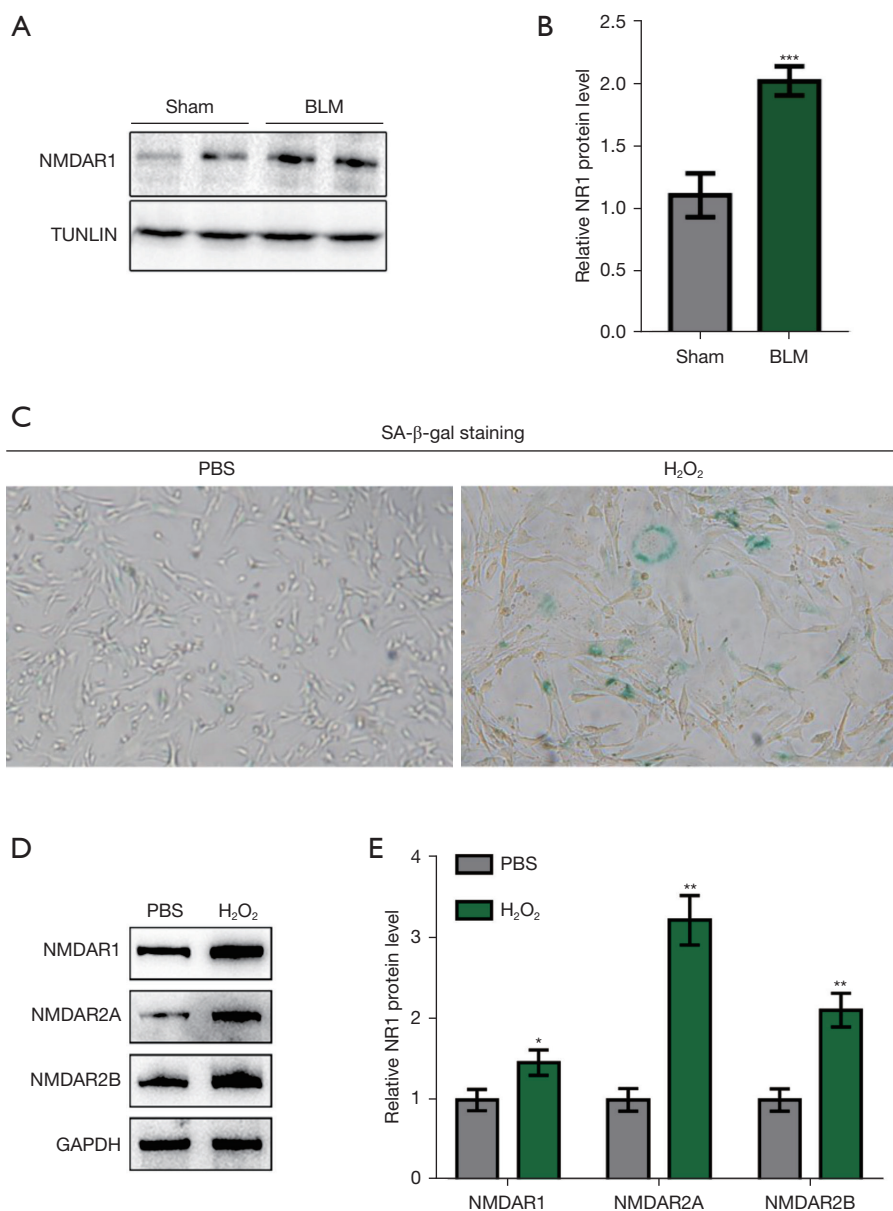


Figure 3 Increased expression of NMDAR subunits was observed in the BLM-induced pulmonary fibrosis model and senescent cell model. (A,B) Expression of NMDAR1 on the primary BM-MSCs of mice in the sham-operated and BLM model groups (n=3); (C) in vitro aging model of purchased primary BM-MSCs induced by hydrogen peroxide, which showed that the positive rate of β-galactosidase staining was significantly higher than that of the control group (×100, n=3); (D,E) the expression levels of NMDAR1, NMDAR2A, and NMDAR2B in the hydrogen peroxide treatment group were considerably higher than those in the control group (n=3). *P<0.05, **P<0.01, ***P<0.0001 vs. Sham. BLM, bleomycin; NMDAR, N-methyl-D-aspartate receptor; SA-β-gal, senescence associated beta-galactosidase; PBS, phosphate buffer solution; GAPDH, glyceraldehyde-3-phosphate dehydrogenase; BM-MSCs, bone marrow mesenchymal stem cells.

(Figure 4G). The protein levels of the pluripotency markers, Oct4 and Nanog, decreased (Figure 4H). In contrast, MK-801 partially increased the expression of ki-67 and hTERT

but also decreased p16 and p21 expression and increased Oct4 and Nanog expression (Figure 4G,4H). Thus, NMDA inhibited BM-MSCs proliferation and cell stemness, and

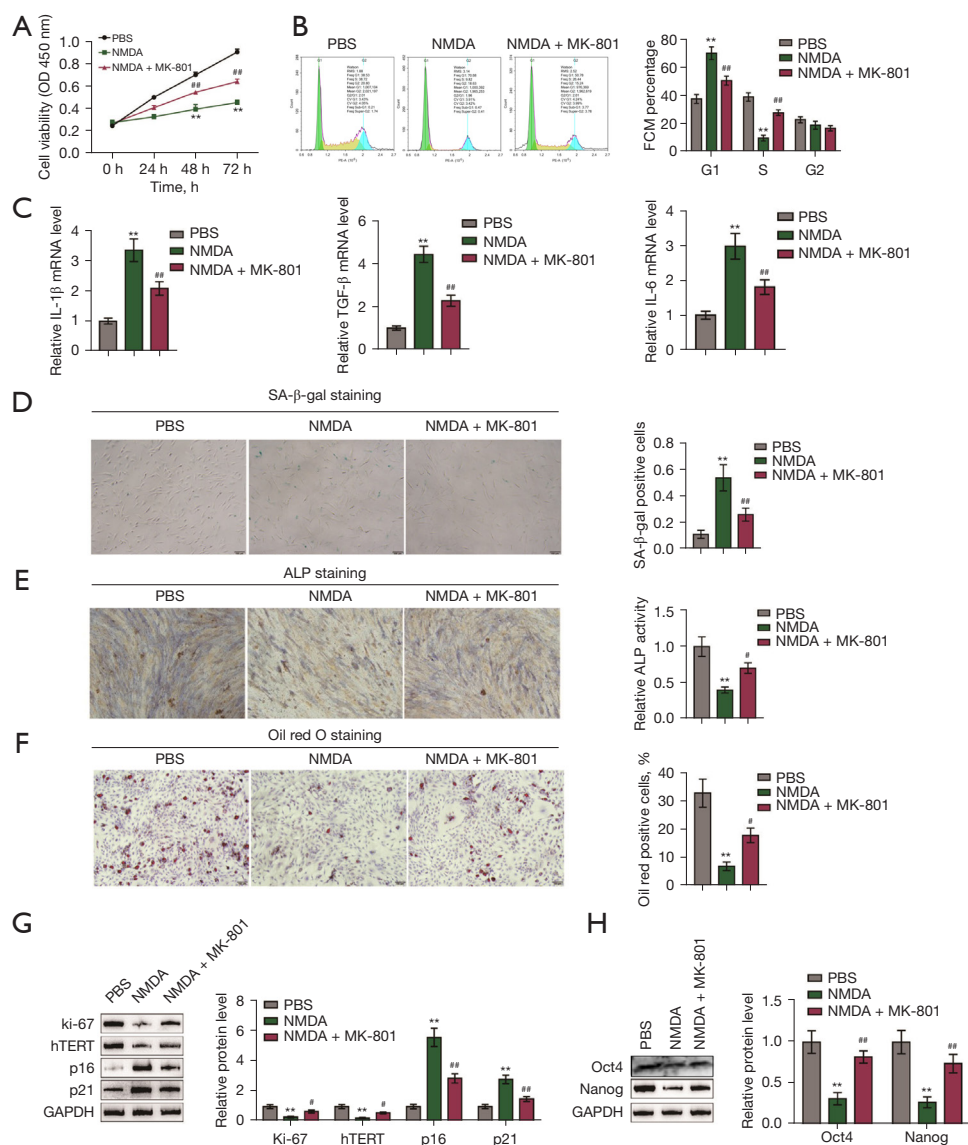


Figure 4 NMDA receptor activation caused BM-MSCs senescence, MK-801 partially ameliorated the senescence of BM-MSCs. (A) Purchased primary mouse BM-MSCs were divided into three groups: PBS, NMDA-treated, and NMDA + MK-801 groups, which received corresponding treatments (see the results section above for the specific treatments). NMDA treatment significantly inhibited the cell viability of BM-MSCs, and MK-801 partially improved cell viability ($n=3$); (B) NMDA treatment arrested the cell cycle of BM-MSCs in the G1 phase, and MK-801 partially improved it ($n=3$); (C) NMDA treatment upregulated IL-1 β , IL-6, and TGF- β mRNA expression, and MK-801 partially inhibited their upregulation ($n=3$); (D) the NMDA-treated group had the highest positive rate of β -galactosidase staining, and MK-801 accelerated aging ($\times 40$, $n=3$); (E,F) ALP staining and oil red O staining were performed for the observation of the osteogenic and adipogenic differentiation ability of BM-MSCs. NMDA treatment inhibited the osteogenic and adipogenic differentiation of BM-MSCs, while MK-801 promoted these processes ($\times 40$, $n=3$); (G) expression levels of proliferation-related proteins (Ki-67 and hTERT) decreased, and the expression levels of aging-related proteins (p16 and p21) in the NMDA treatment group increased. MK-801 partially reduced the expression of Ki-67 and hTERT, and partially increased the expression of P16 and P21 ($n=3$); (H) NMDA treatment decreased the protein levels of the stem cell pluripotency markers, Oct4 and Nanog, which were partially rescued by MK-801 ($n=3$). ** $P < 0.01$ vs. PBS; # $P < 0.05$, ## $P < 0.01$ vs. NMDA. PBS, phosphate buffer solution; NMDA, N-methyl-d-aspartate; MK-801, dizocilpine; FCM, flow cytometry; TGF- β , transforming growth factor beta; IL-1 β , interleukin-1 beta; IL-6, interleukin-6; SA- β -gal, senescence associated beta-galactosidase; ALP, alkaline phosphatase; GAPDH, glyceraldehyde-3-phosphate dehydrogenase; hTERT, human telomerase reverse transcriptase; Oct4, octamer-binding transcription factor 4; BM-MSCs, bone marrow mesenchymal stem cells.

MK-801 partially rescued these processes.

NMDAR activation may act through the Wingless and int-1 (Wnt)/ β -catenin signaling pathway to promote the senescence of BM-MSCs

The Wnt signaling pathway regulates proliferation, differentiation, adhesion, and migration. The two main pathways of WNT signaling include canonical (Wnt/ β -catenin) and non-canonical pathways. In canonical Wnt signaling, β -catenin is a key protein (36). Herein, we investigated the effect of NMDAR activation on Wnt/ β -catenin signaling. BM-MSCs were pretreated with PBS, NMDA, or MK-801, and then NMDA was added (we divided the cells into three groups: PBS, NMDA-treated, and NMDA + MK-801 groups). After each passage, a complete medium containing 3 mM NMDA was used in the NMDA group, while the NMDA + MK-801 group was first pretreated with MK-801 containing 100 μ M for 30 min, and then NMDA was added for the preparation of the final concentration of the medium containing 3 mM NMDA). Cellular proteins were collected and used for the detection of phosphorylation, activity, and nuclear translocation of β -catenin. NMDAR activation significantly promoted β -catenin phosphorylation (Figure 5A), inhibited β -catenin activity (Figure 5A), and inhibited β -catenin nuclear translocation (Figure 5B). Meanwhile, the NMDAR inhibitor, MK-801, partially attenuated the effects of NMDA on β -catenin phosphorylation, activity, and nuclear translocation (Figure 5A,5B). NMDA markedly decreased the protein levels of cyclin D1 and C-myc downstream of the Wnt/ β -catenin pathway, whereas MK-801 partially suppressed downregulation (Figure 5C). These results suggest that NMDA mediates cell senescence by activating the Wnt/ β -catenin pathway, and an NMDA inhibitor can inhibit this process.

NMDA-induced BM-MSCs senescence promotes pulmonary epithelial-mesenchymal transition

Pulmonary fibrosis has long been classified as a type II EMT event (37,38). To further explore the effect of NMDAR activation-mediated senescence of BM-MSCs on pulmonary fibrosis, we observed the effect of BM-MSCs on epithelial cells. BM-MSCs were co-cultured with lung epithelial cells, and the related indicators were examined. First, BM-MSCs were divided into three groups (PBS, NMDA, NMDA + MK-801 groups) for pretreatment. The PBS group was

used as a blank control group for normal passage and medium. The NMDA group was cultured with NMDA complete medium containing 3 mmol/L. The NMDA + MK-801 group was pretreated with MK-801 containing 100 μ mol/L for 30 min following each passage and after the cells adhered to the wall. NMDA was then added so that the final concentration of NMDA in the culture was 3 mmol/L for cultivation (the pretreatment method was the same as that of the fourth part of the experiment).

After β -galactosidase staining, the positive staining rate of cells in the NMDA group was significantly increased. The three groups of BM-MSCs were transferred to the lower layer of the co-culture chamber and co-cultured with the mouse lung epithelial cell line MLE-12 under TGF- β treatment (10 ng/mL, 48 h). The results showed that co-culturing with NMDA-treated BM-MSCs increased the epithelial cell viability (Figure 6A), increased epithelial cell α -SMA, decreased E-cadherin (Figure 6B) and EpCAM, and the expression of vimentin and α -SMA increased (Figure 6C). In contrast, epithelial cells co-cultured with BM-MSCs in the NMDA + MK-801 treatment group showed partially inhibited cell viability (Figure 6A), decreased α -SMA level, and partially increased protein expression levels of E-cadherin and EpCAM (Figure 6B,6C). The expression levels of vimentin and α -SMA were also partially reduced (Figure 6B,6C). Thus, NMDA-treated BM-MSCs promoted EMT in the mouse lung epithelial cell line, MLE-12, whereas MK-801-treated BM-MSCs partially suppressed the development of EMT. We provide a schematic diagram of co-culture (Figure 6D).

Discussion

IPF is a chronic and fatal disease that eventually progresses to respiratory failure. The cause of the disease is unknown, and no curative treatment other than lung transplantation is currently available (1,2). The intratracheal injection of BLM induces pulmonary fibrosis and is a recognized animal model for mimicking the process of IPF. Said *et al.* reported that high concentrations of NMDA (1 mM) can induce acute pulmonary edema in a rat model (39,40), and the same research team further reported that NMDAR inhibitors could alleviate paraquat or xanthine oxidase-induced oxidative lung edema injury, suggesting that NMDAR activation mediates oxidative lung injury (41). Substantial previous data has shown that the intraperitoneal injection of glutamate can induce acute lung injury in mice (42,43). After 3 days of BLM tracheal injection, the content of

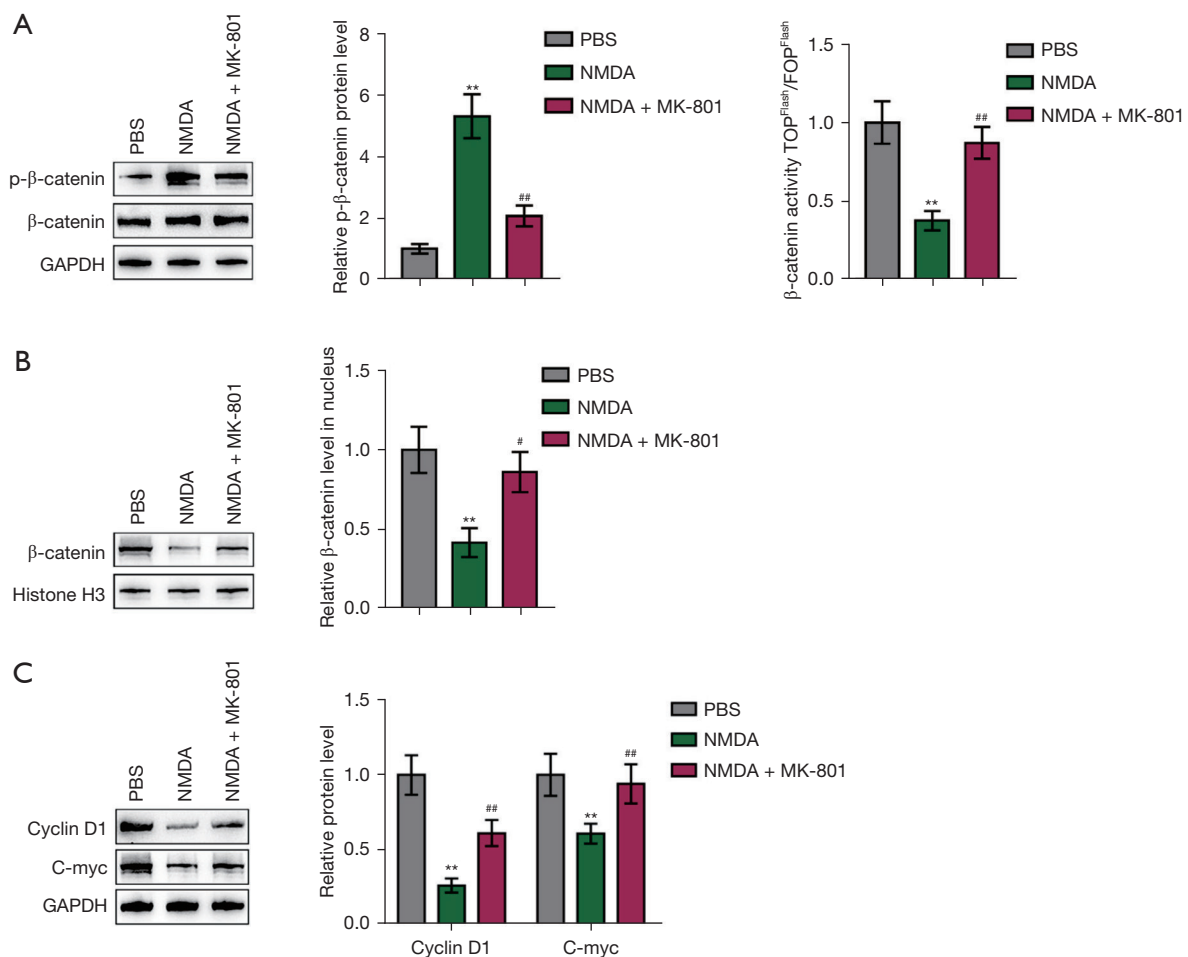


Figure 5 NMDA receptor activation may act through Wnt/ β -catenin signaling pathway to promote the senescence of BM-MSCs. (A) Purchased primary mouse BM-MSCs were divided into three groups: PBS, NMDA-treated, and NMDA + MK-801 groups, which received corresponding treatments. NMDA treatment significantly promoted the phosphorylation of β -catenin and inhibited the activity of β -catenin, which were partially rescued by MK-801 (n=3); (B) NMDA treatment inhibited the nuclear translocation of β -catenin, while MK-801 partially improved it (n=3); (C) the expression of cyclin D1 and C-myc proteins decreased in the NMDA treatment group, which could be partially improved by MK-801 (n=3). ** $P < 0.01$ vs. PBS; # $P < 0.05$, ## $P < 0.01$ vs. NMDA. PBS, phosphate buffer solution; NMDA, N-methyl-d-aspartate; MK-801, dizocilpine; TOP Flash/FOP Flash, commercial firefly luciferase reporter gene; GAPDH, glyceraldehyde-3-phosphate dehydrogenase; BM-MSCs, bone marrow mesenchymal stem cells.

glutamate in bronchoalveolar lavage fluid increases, and memantine alleviates acute lung injury (19). In addition, we confirmed that the NMDAR blocker, memantine, reduces airway inflammation in mice with chronic obstructive pulmonary disease (44). It also plays an important role in other models of acute lung injury, pulmonary fibrosis (45) and intrauterine lung dysplasia (46,47). These findings suggest that endogenous glutamate and NMDAR activation may be involved in various types of acute lung injury, airway inflammation, asthma, and pulmonary fibrosis. In this

study, we extended the duration of memantine treatment. Memantine significantly reduced the extent of pulmonary fibrosis at the peak of pulmonary fibrosis (21 days after BLM intratracheal injection). This result is a continuation of the previous results of our research team, corroborating the theoretical results on the mechanism of NMDARs in lung diseases.

Glutamate (Glu) is the major excitatory neurotransmitter in the central nervous system. Under pathological conditions, extracellular glutamate concentration increases due to

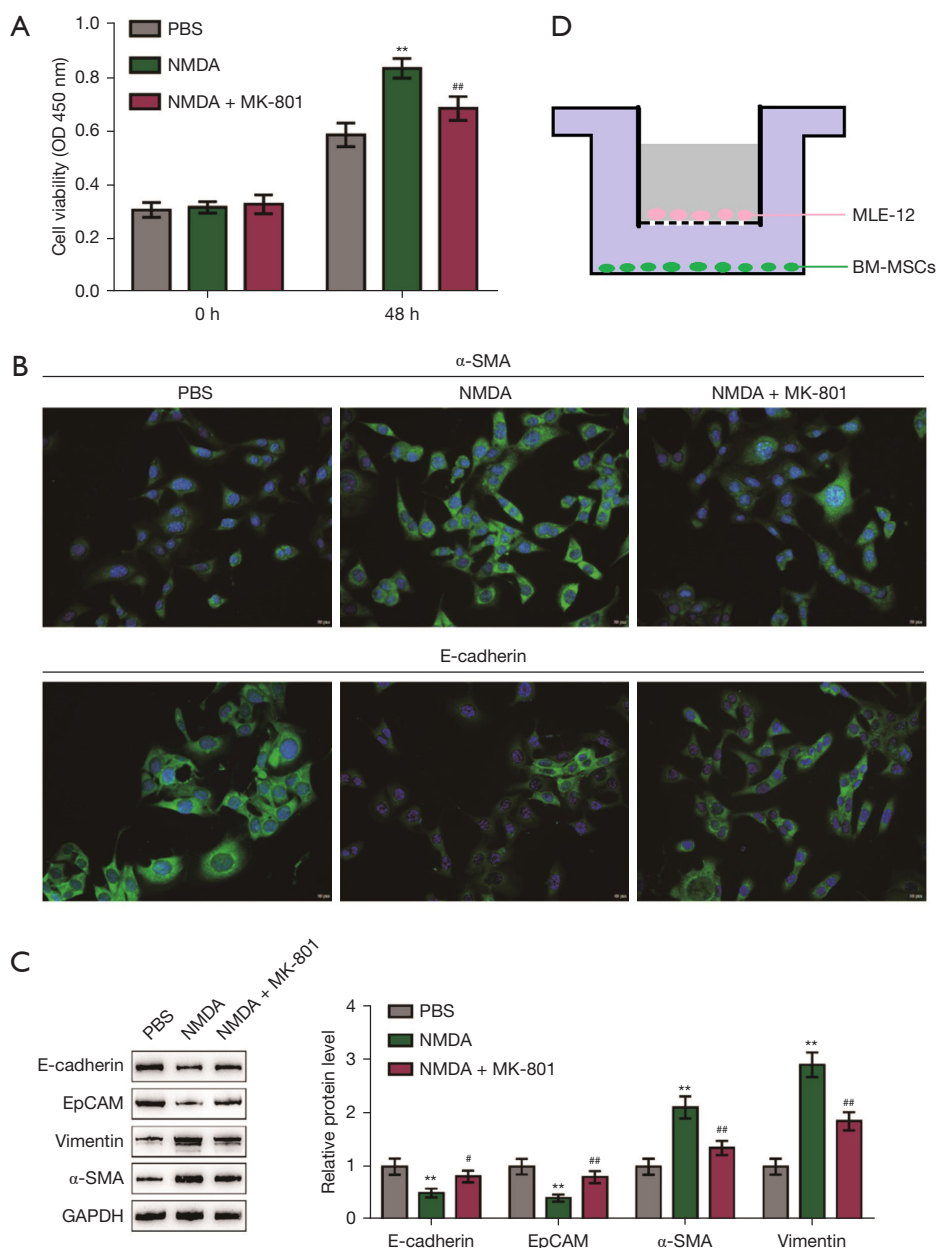


Figure 6 NMDA-induced BM-MSCs senescence promotes pulmonary epithelial-mesenchymal transition. (A) BM-MSCs were divided into three groups (PBS, NMDA, and NMDA + MK-801) for pretreatment (see above for the pretreatment method), and then transferred to the lower layer of the co-culture chamber and the upper layer of MLE-12 cells for co-culturing. BM-MSCs in the NMDA-treated group increased the viability of the MLE-12 cells, and MK-801 partially inhibited this effect (n=3); (B) immunofluorescence staining of MLE-12 cells in three groups showed that BM-MSCs in the NMDA-treated group had increased expression levels of α -SMA and E-cadherin. In the MLE-12 cells, the expression levels decreased, and MK801 partially inhibited this effect ($\times 100$, n=3); (C) three groups of upper MLE-12 cells proteins were collected, and the BM-MSCs in the NMDA-treated group decreased the expression levels of E-cadherin and EpCAM proteins in the MLE-12 cells. The expression levels of vimentin and α -SMA were elevated in the MLE-12 cells, but MK-801 partially inhibited this effect (n=3); (D) schematic diagram of the co-culture of BM-MSCs and MLE-12 cells. **P<0.01 vs. PBS; #P<0.05, ##P<0.01 vs. NMDA. PBS, phosphate buffer solution; NMDA, N-methyl-d-aspartate; MK-801, dizocilpine; MLE-12, mouse lung epithelial cells; BM-MSCs, bone marrow mesenchymal stem cells; EpCAM, epithelial cell adhesion molecule; α -SMA, alpha-smooth muscle actin; GAPDH, glyceraldehyde-3-phosphate dehydrogenase.

abnormal release and clearance. This effect leads to the overstimulation of glutamate receptors, resulting in neuronal cell damage or death, known as excitotoxicity (48). NMDARs are the major receptors that mediate Glu excitotoxicity (49). Our previous study reported for the first time that BM-MSCs express the subunits of NMDARs, and NMDAR activation promotes Ca^{2+} influx in BM-MSCs (17). In a BLM-induced fibrosis model, the content of Glu in the supernatant of BM cells was significantly increased (17). These findings suggest that the release of endogenous Glu may over-activate NMDARs on the membrane of BM-MSCs, leading to excitotoxicity.

BM-MSCs are one of the target cells for NMDAR modulation. However, the physiological significance of NMDAR expression in BM-MSCs remains unclear. The NMDAR1 subunit of the NMDAR is highly expressed in the hippocampus, and the expression of the NMDAR1 protein decreases considerably with age (50). In the central nervous system, Glu treatment can induce senescence in PC12 cells, and memantine reduces oxidative damage and senescence by inhibiting Neuronal Nitric Oxide Synthase (Nnos) activity (51). Alzheimer's disease is one of the most classic aging-related diseases, and memantine has been approved in multiple countries for the treatment of moderate to severe Alzheimer's disease and other central nervous system aging-related diseases (52). This indicates that the role of NMDARs in the mediation of the aging process in the central nervous system is worthy of further study. Meanwhile, the significance of NMDAR expression in BM-MSCs outside the central nervous system remains unclear. The biological implications of increased expression of NMDAR subunits in aging BM-MSCs need to be further clarified. In this study, we further observed that the BM-MSCs of the BLM-induced lung fibrosis model mice were senescent, and the expression of NMDA1, the functional subunit of NMDAR, was significantly higher than that of the control group. We also observed high expression levels of NMDAR subunits in the H202-induced senescence model of BM-MSCs, suggesting that NMDARs are involved in the senescence of BM-MSCs, and NMDARs may be the targets regulating cellular senescence. We proposed the use of BM-MSCs with a high concentration of NMDA (3 mmol/L), which specifically binds to NMDARs and hyperactivates them, thereby mimicking the excitotoxicity produced by the release of endogenous Glu. After NMDAR overactivation, BM-MSCs showed characteristic phenotypes associated with aging (positive β -galactosidase staining, increased expression of aging-related proteins) and affected

functional changes (impaired osteogenic and adipogenic capacity and significant increases in IL-1, IL-6, TGF- β , and other released SASPs).

BM-MSCs transplantation is one of the most promising potential treatments for IPF, and its extensive use and development have been severely limited by the aging phenomenon during its *in vitro* expansion. In this study, we observed for the first time that NMDAR overactivation can induce senescence in BM-MSCs, and the NMDAR inhibitor, MK-801, can partially reverse the senescence phenomenon, providing a new perspective for solving the aging problem of BM-MSCs.

P21 and P16 can deactivate cyclin E- and cyclin D1-related kinase activities at an early stage, thereby inhibiting cell proliferation. P21 and P16 are key molecules in the aging signaling pathway, which suggests that cyclin D1 mediates the aging process (53). Additionally, cyclin D1 has also been found to affect proliferation and differentiation in other stem cells, such as developing hematopoietic stem cells (HSC) (54), adult mammary epithelial stem cells (55), and human embryonic stem cells (56). C-myc is a transcription factor well known for its role in regulating the proliferation, growth, differentiation, and survival of multiple cell types (57). Florea *et al.* observed that after C-myc knockdown, endothelial cells displayed a large and flat morphological appearance and binucleates, underwent gradual cell cycle arrest in the G1 phase, and showed reduced cell proliferation and finally a senescence-related phenotype (58). Elevated levels of the C-myc protein considerably increase the sensitivity of epithelial cells to pro-apoptotic stimuli, such as DNA damage (59). The downregulation of C-myc is essential for cell cycle arrest and the continued survival of cells after DNA damage (60). In the present study, we observed decreased expression of cyclin D1 and C-myc in NMDA-treated BM-MSCs, and this effect was partially ameliorated by the NMDAR inhibitor, MK-801. Moreover, we also found that the phosphorylation level of the Wnt canonical pathway protein, β -catenin, was increased, and MK-801 could partially inhibit this phenomenon. We speculated that NMDAR regulates the expression of cyclin D1 and C-myc via the canonical Wnt signaling pathway, affects the cell cycle, and mediates senescence.

Pulmonary fibrosis has long been classified as a type II EMT event (37,38). Type II EMT is a physiological induction of injury that ceases during tissue repair, wound healing, and regeneration (61). During fibrosis, the persistence of EMT-inducing signals leads to the

accumulation of ECM, which leads to the remodeling of tissue architecture and altered organ pathology (62). The presence or absence of EMT is defined by detecting several biomarkers reflecting the loss of epithelial phenotype and gain of mesenchymal phenotype, namely, proteins involved in cell contact (loss of E-cadherin and gain of N-cadherin), cytoskeletal proteins (loss of cytokeratin and vimentin and increased α -SMA, desmin, and fibronectin), and luminal proteins secreted by blast cells (increased ECM or metalloproteinase secretion) (63).

TGF- β is one of the most studied growth factors involved in EMT and a key molecule that activates the fibrotic program (64,65). IL-1 β and IL-6 are involved in the EMT process; IL-1 β can act through the mitogen-activated protein kinases (MAPK) signaling pathway to enhance TGF- β 1-induced EMT (66). All-trans retinoic acid inhibits EMT by downregulating IL-6 in endometriosis (67). In our study, after high concentrations of NMDA-treated BM-MSCs were added, the cells senesced, and the senescent cells released SASP factors (TGF- β , IL-1 β , and IL-6) during co-culture with MLE-12 cells. TGF- β , IL-1 β , and IL-6 in the cell supernatant promoted the occurrence of EMT in the MLE-12 cells. Therefore, through the immunofluorescence results, we observed that by co-culturing with NMDA-treated BM-MSCs, the expression of the epithelial marker (E-cadherin) decreased, whereas the expression of the mesenchymal marker (α -SMA) increased in MLE-12 cells. MK-801 partially improved the above phenomenon, and we observed the same phenomenon in the WB results.

In the classical Wnt signaling pathway, Wnt1-like ligands initiate signaling cascades after binding to the seven-transmembrane frizzled receptor family and the low-density lipoprotein receptor-related protein family (LRP5/6). β -catenin is a key protein in this signaling pathway. When glycogen synthase kinase 3 β expression is inhibited, β -catenin increases steadily and gradually accumulates, and β -catenin then translocates to the nucleus to produce biological effects. In contrast, unstable β -catenin is phosphorylated in the cytoplasm and is inactive. Wnts are the growth stimulators of the Wnt pathway and lead to cell proliferation, and Wnt signaling affects the cell cycle at various stages (36). A reduction in canonical Wnt activity has been found in the hippocampus of aged animals; Wnt3 expression in hippocampal astrocytes and the number of Wnt3-secreting astrocytes decrease during aging (68). Fifteen Wnt proteins are regulated to varying degrees in the kidneys of aged mice. With the progression of aging, the active form of β -catenin and the total protein expression level are significantly

upregulated (69). Notum is a Wnt pathway inhibitor; the secretion of Notum increases in senescent Paneth cells, whereas Wnt gene expression decreases (70). These results suggest that the Wnt signaling pathway mediates the aging process but may play a role in promoting or inhibiting aging in different organs. Our study showed that NMDAR activation downregulated β -catenin protein activity and mediated the aging of BM-MSCs.

There are many concerns about MSCs treatment for IPF. Concerns about MSCs therapy may be related to their potential to enhance pulmonary fibrosis. Although a study has shown the possibility of fibroblasts (MSC subsets circulating in the blood) differentiating into fibroblasts/myofibroblasts (71). Increased levels of MSCs in bronchoalveolar lavage (BAL) fluid are predictors of bronchiolitis obliterans in transplanted lungs (72). However, AETHER confirmed the safety of hMSCs in IPF patients with 2×10^8 cells per infusion (7). In a clinical trial of moderate to severe IPF patients, Averyanov *et al.* found that IPF patients in the treatment group received 1.6×10^9 MSCs (the highest number of stem cells ever recorded) intravenously for 52 weeks, and found significant improvement in 6-minute exercise test and lung function. But the placebo group showed a progressive decline in lung function. The treatment group had no obvious adverse reactions except for a brief fever on the first day (73). In another study of moderate and severe IPF, good safety and efficacy of intravenous MSCs were also observed (74). It has even been reported that intratracheal injection of MSCs for mild and moderate IPF is safe and effective (75). Therefore, the safety, tolerability, and potential benefits of high-dose MSCs therapy for IPF are significant. However, the optimal source, route, frequency and timing of MSCs administration need to be further explored. Concerns about the risks of BM donation, the possibility of IPF deterioration caused by MSCs intervention, and the adverse effects of biopsy on lung function persist. MSCs are safely used in patients with IPF, but large multicenter randomized trials are still needed.

Research on the relationship between BM-MSCs and pulmonary fibrosis has mainly focused on the effect of exogenous BM-MSCs in the treatment of pulmonary fibrosis and related mechanisms, as well as how the function of BM-MSCs changes in pulmonary fibrosis. However, the mechanism and significance of the changes are rarely studied. When exogenous BM-MSCs were used to treat pulmonary fibrosis, BM-MSCs were transfected with an adenovirus vector carrying a green fluorescent protein (GFP) reporter gene (Ad-GFP), and these cells were

transplanted into small cells via tail vein injection 7 days after paraquat injection. In mice, the number of BM-MSCs recruited in the lung tissues of paraquat-intoxicated mice was significantly higher than that in mice injected with normal saline (76). In GFP BM chimera mice, BM-derived GFP-positive cells in BLM-induced pulmonary fibrosis were abundant in the lung tissues compared with the control group, and these GFP-positive cells exhibited an epithelial phenotype (77). This suggests that both endogenous BM-MSCs and transplanted exogenous BM-MSCs return to the damaged tissue. But the details of its role and mechanism are not very clear. BM is a reservoir for various stem cell populations. When the body is injured, stem cells in BM can be mobilized to different degrees into the peripheral blood circulation. Endogenous BM-MSCs from BM can also be mobilized into damaged tissues from the circulatory system to participate in the repair and regeneration of damaged tissues (78). It has been reported that the expression of cytokines and chemokine receptors of BM-MSCs in aged mice decreased, which reduced the activity of BM-MSCs migrating to the injury site and weakened their protective effect on lung tissues (79,80). The effect of senescence on the chemotactic homing of BM-MSCs to damaged lung tissue still needs to be further studied. Rojas *et al.* reported that before the BLM-induced pulmonary fibrosis mouse model was used, the BM was inhibited with busulfan, and the degree of pulmonary fibrosis was aggravated. Even if exogenous BM-MSCs transplantation can reduce pulmonary fibrosis, the degree of pulmonary fibrosis remains higher than that of mice with normal BM function (81). In our previous study, we found that the prophylactic administration of granulocyte-colony stimulating factor (G-CSF) for the mobilization of BM cells has a protective effect on BLM-induced pulmonary fibrosis (82). G-CSF can mobilize BM-MSCs to infiltrate into the brain of Mice with Alzheimer's disease through stromal cell-derived factor 1/C-X-C chemokine receptor type 4 (SDF-1/CXCR4) chemotactic signaling axis and supplement neural lineage cells (83). The mobilization of endogenous BM-MSCs can be one of the important ways to prevent and treat pulmonary fibrosis. Senescence of the endogenous BM-MSCs was observed during BLM-induced pulmonary fibrosis. The senescence may be related to the activation of NMDARs. Therefore, we speculate that improving the senescence of endogenous BM-MSCs may also be one of the targets for prevention and treatment of pulmonary fibrosis. Aging BM-MSCs secrete a large amount of SASP, which adversely affects the cellular microenvironment and

neighboring cells. Look for the factor most closely related to pulmonary fibrosis among the SASP components. By inhibiting its secretion or blocking its action, it is also possible to achieve anti-pulmonary fibrosis effect. Our results showed that the functional status of BM has a huge impact on the prognosis of BLM-induced pulmonary fibrosis in mice. In general, BLM is a chemotherapeutic drug. We used its side effects to establish a pulmonary fibrosis model. BLM has a suppressive effect on BM. In the follow-up experiments, we will supplement the *in vitro* experiments to investigate the effect of BLM on BM-MSCs. We speculated that in the BLM-induced lung fibrosis model, BLM inhibits the normal function of the BM. BM-MSCs age during pulmonary fibrosis, and the aged BM-MSCs are partially recruited into damaged lung tissues and cannot differentiate into normal alveolar epithelium. Moreover, aging BM-MSCs secrete SASP factors, which promote EMT in epithelial cells and aggravate pulmonary fibrosis. The NMDAR inhibitors, memantine and MK-801, may be used as targets to accelerate the aging of BM-MSCs, inhibit the occurrence of EMT, and improve pulmonary fibrosis, but the specific steps and mechanisms need to be determined in future studies. It has been previously reported that IPF and primary lung cancer are closely related; they share pathogenic similarities in genetic and epigenetic markers and may even share common pathogenesis and molecular pathways (84,85). Thus, identifying common therapeutic targets for IPF and lung cancer may be a possible direction for our follow-up experiments.

MSCs are not only capable of senescence when expanded *in vitro*, but also *in vivo*. This senescence is due to the age of the host, as well as obesity, inflammatory state and disease state of the host (86,87). When the host state is good, the main function of MSCs in adult tissues is to maintain tissue homeostasis, play anti-inflammatory and immunomodulatory roles. During *in vivo* aging, the clonal composition of the stem cell pool changes, which may affect the composition and function of tissues (88), leading to progressive depletion of the stem cell pool, gradual reduction of self-renewal potential, and ultimately tissue and organ dysfunction (89). For example, BM-MSCs aging is responsible for impaired fracture healing. Aging of BM-MSCs *in vivo* means reduced osteogenic ability, which leads to age-related diseases, such as osteoporosis (90). Aging of BM-MSCs can also lead to impaired hematopoietic function. BM-MSCs from elderly donors (the basis of maintaining HSC cells in BM) can activate SASP, make HSC in an inflammatory state, and decrease hematopoietic function (91). Aging of the synovial

and subchondral BM-MSCs may lead to joint changes and the development of osteoarthritis (92). Geroscience hypothesis (93) states that most aging-related diseases are caused by common and closely related diseases, including chronic low-grade inflammation, macromolecule/organelle dysfunction, stem cell dysfunction and accumulation of senescent cells. Senescent BM-MSCs *in vivo* can lose their ability to self-renew and protect the body and even aggravate the progression of diseases through releasing excessive reactive oxygen species (ROS) (94), increasing autophagy (95), epigenetic changes (96), activation of SASP (97) and other pathways (98).

There are still many deficiencies. We did not use blockers in the *in vitro* aging model of BM-MSCs induced by hydrogen peroxide, and observed the expression changes of NMDARs after blocking. We did not use viruses to knock down NMDARs on BM-MSCs membranes to further confirm the role of NMDARs in hydrogen peroxide induced senescence. We only observed changes in the expression of WNT signaling proteins during NMDA-induced aging of BM-MSCs. To observe whether NMDAR activation can induce senescence without the use of WNT signaling pathway blockers or agonists. Moreover, the connection point between downstream signaling molecules of NMDAR and WNT signaling pathway has not been found, which needs to be further improved in our follow-up work.

Acknowledgments

Funding: This work was supported by the National Natural Science Foundation of China (Nos. 81870059; 82070068; 81900070), the Natural Science Foundation of Hunan Province (No. 2020JJ5813), and the Changsha Science and Technology (No. Kq1907026).

Footnote

Reporting Checklist: The authors have completed the ARRIVE reporting checklist. Available at <https://atm.amegroups.com/article/view/10.21037/atm-22-2507/rc>

Data Sharing Statement: Available at <https://atm.amegroups.com/article/view/10.21037/atm-22-2507/dss>

Conflicts of Interest: All authors have completed the ICMJE uniform disclosure form (available at <https://atm.amegroups.com/article/view/10.21037/atm-22-2507/coif>).

The authors have no conflicts of interest to declare.

Ethical Statement: The authors are accountable for all aspects of the work and ensure that questions related to the accuracy or integrity of any part of the work are appropriately investigated and resolved. Animal experiments were performed under a project license (No. 2019-121) granted by the Ethics Committee of Central South University (Changsha, China) and were performed in accordance with the guidelines of the National Institutes of Health (NIH) for the care and use of animals.

Open Access Statement: This is an Open Access article distributed in accordance with the Creative Commons Attribution-NonCommercial-NoDerivs 4.0 International License (CC BY-NC-ND 4.0), which permits the non-commercial replication and distribution of the article with the strict proviso that no changes or edits are made and the original work is properly cited (including links to both the formal publication through the relevant DOI and the license). See: <https://creativecommons.org/licenses/by-nc-nd/4.0/>.

References

1. Richeldi L, Collard HR, Jones MG. Idiopathic pulmonary fibrosis. *Lancet* 2017;389:1941-52.
2. Kumar A, Kapnadak SG, Girgis RE, et al. Lung transplantation in idiopathic pulmonary fibrosis. *Expert Rev Respir Med* 2018;12:375-85.
3. Li X, Yue S, Luo Z. Mesenchymal stem cells in idiopathic pulmonary fibrosis. *Oncotarget* 2017;8:102600-16.
4. Yu SH, Liu LJ, Lv B, et al. Inhibition of bleomycin-induced pulmonary fibrosis by bone marrow-derived mesenchymal stem cells might be mediated by decreasing MMP9, TIMP-1, INF- γ and TGF- β . *Cell Biochem Funct* 2015;33:356-66.
5. Wang ZC, Yang S, Huang JJ, et al. Effect of bone marrow mesenchymal stem cells on the Smad expression of hepatic fibrosis rats. *Asian Pac J Trop Med* 2014;7:321-4.
6. Ortiz LA, Gambelli F, McBride C, et al. Mesenchymal stem cell engraftment in lung is enhanced in response to bleomycin exposure and ameliorates its fibrotic effects. *Proc Natl Acad Sci U S A* 2003;100:8407-11.
7. Glassberg MK, Minkiewicz J, Toonkel RL, et al. Allogeneic Human Mesenchymal Stem Cells in Patients With Idiopathic Pulmonary Fibrosis via Intravenous Delivery (AETHER): A Phase I Safety Clinical Trial. *Chest* 2017;151:971-81.

8. Khouri NF, Saral R, Armstrong EM, et al. Pulmonary interstitial changes following bone marrow transplantation. *Radiology* 1979;133:587-92.
9. Prockop DJ. Marrow stromal cells as stem cells for nonhematopoietic tissues. *Science* 1997;276:71-4.
10. Herzog EL, Chai L, Krause DS. Plasticity of marrow-derived stem cells. *Blood* 2003;102:3483-93.
11. Park D, Spencer JA, Koh BI, et al. Endogenous bone marrow MSCs are dynamic, fate-restricted participants in bone maintenance and regeneration. *Cell Stem Cell* 2012;10:259-72.
12. Cárdenas N, Álvarez D, Sellarés J, et al. Senescence of bone marrow-derived mesenchymal stem cells from patients with idiopathic pulmonary fibrosis. *Stem Cell Res Ther* 2018;9:257.
13. Lipton SA. Paradigm shift in neuroprotection by NMDA receptor blockade: memantine and beyond. *Nat Rev Drug Discov* 2006;5:160-70.
14. Griffin WC 3rd, Haun HL, Hazelbaker CL, et al. Increased extracellular glutamate in the nucleus accumbens promotes excessive ethanol drinking in ethanol dependent mice. *Neuropsychopharmacology* 2014;39:707-17.
15. Dickman KG, Youssef JG, Mathew SM, et al. Ionotropic glutamate receptors in lungs and airways: molecular basis for glutamate toxicity. *Am J Respir Cell Mol Biol* 2004;30:139-44.
16. Gono T, Mizuno N, Inagaki N, et al. Functional neuronal ionotropic glutamate receptors are expressed in the non-neuronal cell line MIN6. *J Biol Chem* 1994;269:16989-92.
17. Li X, Li C, Tang Y, et al. NMDA receptor activation inhibits the antifibrotic effect of BM-MSCs on bleomycin-induced pulmonary fibrosis. *Am J Physiol Lung Cell Mol Physiol* 2018;315:L404-21.
18. Abbaszadeh S, Javidmehr A, Askari B, et al. Memantine, an NMDA receptor antagonist, attenuates cardiac remodeling, lipid peroxidation and neutrophil recruitment in heart failure: A cardioprotective agent? *Biomed Pharmacother* 2018;108:1237-43.
19. Li Y, Liu Y, Peng X, et al. NMDA Receptor Antagonist Attenuates Bleomycin-Induced Acute Lung Injury. *PLoS One* 2015;10:e0125873.
20. Peng X, Li X, Li C, et al. NMDA receptor activation inhibits the protective effect of BM-MSCs on bleomycin-induced lung epithelial cell damage by inhibiting ERK signaling and the paracrine factor HGF. *Int J Mol Med* 2019;44:227-39.
21. Yue Y, Luo Z, Liao Z, et al. Excessive activation of NMDA receptor inhibits the protective effect of endogenous bone marrow mesenchymal stem cells on promoting alveolarization in bronchopulmonary dysplasia. *Am J Physiol Cell Physiol* 2019;316:C815-27.
22. López-Otín C, Blasco MA, Partridge L, et al. The hallmarks of aging. *Cell* 2013;153:1194-217.
23. Campisi J, Andersen JK, Kapahi P, et al. Cellular senescence: a link between cancer and age-related degenerative disease? *Semin Cancer Biol* 2011;21:354-9.
24. He S, Sharpless NE. Senescence in Health and Disease. *Cell* 2017;169:1000-11.
25. Storer M, Mas A, Robert-Moreno A, et al. Senescence is a developmental mechanism that contributes to embryonic growth and patterning. *Cell* 2013;155:1119-30.
26. Demaria M, Ohtani N, Youssef SA, et al. An essential role for senescent cells in optimal wound healing through secretion of PDGF-AA. *Dev Cell* 2014;31:722-33.
27. van Deursen JM. The role of senescent cells in ageing. *Nature* 2014;509:439-46.
28. Le Boulch M, Ahmed EK, Rogowska-Wrzesinska A, et al. Proteome oxidative carbonylation during oxidative stress-induced premature senescence of WI-38 human fibroblasts. *Mech Ageing Dev* 2018;170:59-71.
29. Ashcroft T, Simpson JM, Timbrell V. Simple method of estimating severity of pulmonary fibrosis on a numerical scale. *J Clin Pathol* 1988;41:467-70.
30. Friedenstein AJ, Chailakhyan RK, Latsinik NV, et al. Stromal cells responsible for transferring the microenvironment of the hemopoietic tissues. Cloning in vitro and retransplantation in vivo. *Transplantation* 1974;17:331-40.
31. Dominici M, Le Blanc K, Mueller I, et al. Minimal criteria for defining multipotent mesenchymal stromal cells. The International Society for Cellular Therapy position statement. *Cytotherapy* 2006;8:315-7.
32. Boyer LA, Lee TI, Cole MF, et al. Core transcriptional regulatory circuitry in human embryonic stem cells. *Cell* 2005;122:947-56.
33. Tsai CC, Su PF, Huang YF, et al. Oct4 and Nanog directly regulate Dnmt1 to maintain self-renewal and undifferentiated state in mesenchymal stem cells. *Mol Cell* 2012;47:169-82.
34. Jie MM, Chang X, Zeng S, et al. Diverse regulatory manners of human telomerase reverse transcriptase. *Cell Commun Signal* 2019;17:63.
35. Zhang L, Li Y, Guan CY, et al. Therapeutic effect of human umbilical cord-derived mesenchymal stem cells on injured rat endometrium during its chronic phase. *Stem Cell Res Ther* 2018;9:36.

36. Nusse R, Clevers H. Wnt/ β -Catenin Signaling, Disease, and Emerging Therapeutic Modalities. *Cell* 2017;169:985-99.
37. Salton F, Volpe MC, Confalonieri M. Epithelial-Mesenchymal Transition in the Pathogenesis of Idiopathic Pulmonary Fibrosis. *Medicina (Kaunas)* 2019;55:83.
38. Thiery JP, Acloque H, Huang RY, et al. Epithelial-mesenchymal transitions in development and disease. *Cell* 2009;139:871-90.
39. Said SI, Berisha HI, Pakbaz H. Excitotoxicity in the lung: N-methyl-D-aspartate-induced, nitric oxide-dependent, pulmonary edema is attenuated by vasoactive intestinal peptide and by inhibitors of poly(ADP-ribose) polymerase. *Proc Natl Acad Sci U S A* 1996;93:4688-92.
40. Said SI, Pakbaz H, Berisha HI, et al. NMDA receptor activation: critical role in oxidant tissue injury. *Free Radic Biol Med* 2000;28:1300-2.
41. Mailliet I, Perche O, Pâris A, et al. Glufosinate aerogenic exposure induces glutamate and IL-1 receptor dependent lung inflammation. *Clin Sci (Lond)* 2016;130:1939-54.
42. Taylor JD. COPD and the response of the lung to tobacco smoke exposure. *Pulm Pharmacol Ther* 2010;23:376-83.
43. Shen L, Han JZ, Li C, et al. Protective effect of ginsenoside Rg1 on glutamate-induced lung injury. *Acta Pharmacol Sin* 2007;28:392-7.
44. Cheng Q, Fang L, Feng D, et al. Memantine ameliorates pulmonary inflammation in a mice model of COPD induced by cigarette smoke combined with LPS. *Biomed Pharmacother* 2019;109:2005-2013.
45. Wang Y, Yue S, Luo Z, et al. N-methyl-D-aspartate receptor activation mediates lung fibroblast proliferation and differentiation in hyperoxia-induced chronic lung disease in newborn rats. *Respir Res* 2016;17:136.
46. Liao Z, Zhou X, Luo Z, et al. N-Methyl-D-aspartate Receptor Excessive Activation Inhibited Fetal Rat Lung Development In Vivo and In Vitro. *Biomed Res Int* 2016;2016:5843981.
47. Wang M, Luo Z, Liu S, et al. Glutamate mediates hyperoxia-induced newborn rat lung injury through N-methyl-D-aspartate receptors. *Am J Respir Cell Mol Biol* 2009;40:260-7.
48. Choi DW. Ionic dependence of glutamate neurotoxicity. *J Neurosci* 1987;7:369-79.
49. Papouin T, Ladépêche L, Ruel J, et al. Synaptic and extrasynaptic NMDA receptors are gated by different endogenous coagonists. *Cell* 2012;150:633-46.
50. Kumar A, Foster TC. Alteration in NMDA Receptor Mediated Glutamatergic Neurotransmission in the Hippocampus During Senescence. *Neurochem Res* 2019;44:38-48.
51. Ota H, Ogawa S, Ouchi Y, et al. Protective effects of NMDA receptor antagonist, memantine, against senescence of PC12 cells: A possible role of nNOS and combined effects with donepezil. *Exp Gerontol* 2015;72:109-16.
52. Guo J, Wang Z, Liu R, et al. Memantine, Donepezil, or Combination Therapy-What is the best therapy for Alzheimer's Disease? A Network Meta-Analysis. *Brain Behav* 2020;10:e01831.
53. Stein GH, Drullinger LF, Soulard A, et al. Differential roles for cyclin-dependent kinase inhibitors p21 and p16 in the mechanisms of senescence and differentiation in human fibroblasts. *Mol Cell Biol* 1999;19:2109-17.
54. Chaves-Ferreira M, Krenn G, Vasseur F, et al. The cyclin D1 carboxyl regulatory domain controls the division and differentiation of hematopoietic cells. *Biol Direct* 2016;11:21.
55. Jeselsohn R, Brown NE, Arendt L, et al. Cyclin D1 kinase activity is required for the self-renewal of mammary stem and progenitor cells that are targets of MMTV-ErbB2 tumorigenesis. *Cancer Cell* 2010;17:65-76.
56. Pauklin S, Madrigal P, Bertero A, et al. Initiation of stem cell differentiation involves cell cycle-dependent regulation of developmental genes by Cyclin D. *Genes Dev* 2016;30:421-33.
57. Pelengaris S, Khan M. The many faces of c-MYC. *Arch Biochem Biophys* 2003;416:129-36.
58. Florea V, Bhagavatula N, Simovic G, et al. c-Myc is essential to prevent endothelial pro-inflammatory senescent phenotype. *PLoS One* 2013;8:e73146.
59. Maclean KH, Keller UB, Rodriguez-Galindo C, et al. c-Myc augments gamma irradiation-induced apoptosis by suppressing Bcl-XL. *Mol Cell Biol* 2003;23:7256-70.
60. Cannell IG, Kong YW, Johnston SJ, et al. p38 MAPK/MK2-mediated induction of miR-34c following DNA damage prevents Myc-dependent DNA replication. *Proc Natl Acad Sci U S A* 2010;107:5375-80.
61. Kalluri R, Weinberg RA. The basics of epithelial-mesenchymal transition. *J Clin Invest* 2009;119:1420-8.
62. Kalluri R, Neilson EG. Epithelial-mesenchymal transition and its implications for fibrosis. *J Clin Invest* 2003;112:1776-84.
63. Pain M, Bermudez O, Lacoste P, et al. Tissue remodelling in chronic bronchial diseases: from the epithelial to mesenchymal phenotype. *Eur Respir Rev* 2014;23:118-30.
64. Zhang C, Zhu X, Hua Y, et al. YY1 mediates TGF- β 1-induced EMT and pro-fibrogenesis in alveolar epithelial

- cells. *Respir Res* 2019;20:249.
65. Kim KK, Sheppard D, Chapman HA. TGF- β 1 Signaling and Tissue Fibrosis. *Cold Spring Harb Perspect Biol* 2018;10:a022293.
 66. Zhang S, Fan Y, Qin L, et al. IL-1 β augments TGF- β inducing epithelial-mesenchymal transition of epithelial cells and associates with poor pulmonary function improvement in neutrophilic asthmatics. *Respir Res* 2021;22:216.
 67. Li L, Gao H, Pan L, et al. All-trans retinoic acid inhibits epithelial-to-mesenchymal transition (EMT) through the down-regulation of IL-6 in endometriosis. *Ann Palliat Med* 2021;10:11348-61.
 68. Gómez-Oliva R, Geribaldi-Doldán N, Domínguez-García S, et al. Vitamin D deficiency as a potential risk factor for accelerated aging, impaired hippocampal neurogenesis and cognitive decline: a role for Wnt/ β -catenin signaling. *Aging (Albany NY)* 2020;12:13824-44.
 69. Miao J, Liu J, Niu J, et al. Wnt/ β -catenin/RAS signaling mediates age-related renal fibrosis and is associated with mitochondrial dysfunction. *Aging Cell* 2019;18:e13004.
 70. Penttinmikko N, Iqbal S, Mana M, et al. Notum produced by Paneth cells attenuates regeneration of aged intestinal epithelium. *Nature* 2019;571:398-402.
 71. Andersson-Sjöland A, de Alba CG, Nihlberg K, et al. Fibrocytes are a potential source of lung fibroblasts in idiopathic pulmonary fibrosis. *Int J Biochem Cell Biol* 2008;40:2129-40.
 72. Badri L, Murray S, Liu LX, et al. Mesenchymal stromal cells in bronchoalveolar lavage as predictors of bronchiolitis obliterans syndrome. *Am J Respir Crit Care Med* 2011;183:1062-70.
 73. Averyanov A, Koroleva I, Konoplyannikov M, et al. First-in-human high-cumulative-dose stem cell therapy in idiopathic pulmonary fibrosis with rapid lung function decline. *Stem Cells Transl Med* 2020;9:6-16.
 74. Tzouveleki A, Paspaliaris V, Koliakos G, et al. A prospective, non-randomized, no placebo-controlled, phase Ib clinical trial to study the safety of the adipose derived stromal cells-stromal vascular fraction in idiopathic pulmonary fibrosis. *J Transl Med* 2013;11:171.
 75. Chambers DC, Enever D, Ilic N, et al. A phase 1b study of placenta-derived mesenchymal stromal cells in patients with idiopathic pulmonary fibrosis. *Respirology* 2014;19:1013-8.
 76. Chen J, Si L, Zhou L, et al. Role of bone marrow mesenchymal stem cells in the development of PQ-induced pulmonary fibrosis. *Mol Med Rep* 2019;19:3283-90.
 77. Hashimoto N, Jin H, Liu T, et al. Bone marrow-derived progenitor cells in pulmonary fibrosis. *J Clin Invest* 2004;113:243-52.
 78. Frenette PS, Pinho S, Lucas D, et al. Mesenchymal stem cell: keystone of the hematopoietic stem cell niche and a stepping-stone for regenerative medicine. *Annu Rev Immunol* 2013;31:285-316.
 79. Bustos ML, Huleihel L, Kapetanaki MG, et al. Aging mesenchymal stem cells fail to protect because of impaired migration and antiinflammatory response. *Am J Respir Crit Care Med* 2014;189:787-98.
 80. Yang S, Liu P, Jiang Y, et al. Therapeutic Applications of Mesenchymal Stem Cells in Idiopathic Pulmonary Fibrosis. *Front Cell Dev Biol* 2021;9:639657.
 81. Rojas M, Xu J, Woods CR, et al. Bone marrow-derived mesenchymal stem cells in repair of the injured lung. *Am J Respir Cell Mol Biol* 2005;33:145-52.
 82. Zhao FY, Cheng TY, Yang L, et al. G-CSF Inhibits Pulmonary Fibrosis by Promoting BMSC Homing to the Lungs via SDF-1/CXCR4 Chemotaxis. *Sci Rep* 2020;10:10515.
 83. Wu CC, Wang IF, Chiang PM, et al. G-CSF-mobilized Bone Marrow Mesenchymal Stem Cells Replenish Neural Lineages in Alzheimer's Disease Mice via CXCR4/SDF-1 Chemotaxis. *Mol Neurobiol* 2017;54:6198-212.
 84. Kinoshita T, Goto T. Molecular Mechanisms of Pulmonary Fibrogenesis and Its Progression to Lung Cancer: A Review. *Int J Mol Sci* 2019;20:1461.
 85. Tzouveleki A, Gomatou G, Bouros E, et al. Common Pathogenic Mechanisms Between Idiopathic Pulmonary Fibrosis and Lung Cancer. *Chest* 2019;156:383-91.
 86. Franceschi C, Garagnani P, Parini P, et al. Inflammaging: a new immune-metabolic viewpoint for age-related diseases. *Nat Rev Endocrinol* 2018;14:576-90.
 87. Frasca D, Blomberg BB, Paganelli R. Aging, Obesity, and Inflammatory Age-Related Diseases. *Front Immunol* 2017;8:1745.
 88. Behrens A, van Deursen JM, Rudolph KL, et al. Impact of genomic damage and ageing on stem cell function. *Nat Cell Biol* 2014;16:201-7.
 89. McHugh D, Gil J. Senescence and aging: Causes, consequences, and therapeutic avenues. *J Cell Biol* 2018;217:65-77.
 90. Wagner DR, Karnik S, Gunderson ZJ, et al. Dysfunctional stem and progenitor cells impair fracture healing with age. *World J Stem Cells* 2019;11:281-96.
 91. Gnani D, Crippa S, Della Volpe L, et al. An early-senescence state in aged mesenchymal stromal cells

- contributes to hematopoietic stem and progenitor cell clonogenic impairment through the activation of a pro-inflammatory program. *Aging Cell* 2019;18:e12933.
92. Malaise O, Tachikart Y, Constantinides M, et al. Mesenchymal stem cell senescence alleviates their intrinsic and seno-suppressive paracrine properties contributing to osteoarthritis development. *Aging (Albany NY)* 2019;11:9128-46.
 93. Kennedy BK, Berger SL, Brunet A, et al. Geroscience: linking aging to chronic disease. *Cell* 2014;159:709-13.
 94. Fafián-Labora JA, Morente-López M, Arufe MC. Effect of aging on behaviour of mesenchymal stem cells. *World J Stem Cells* 2019;11:337-46.
 95. Ma Y, Qi M, An Y, et al. Autophagy controls mesenchymal stem cell properties and senescence during bone aging. *Aging Cell* 2018;17:e12709.
 96. Franzen J, Zirkel A, Blake J, et al. Senescence-associated DNA methylation is stochastically acquired in subpopulations of mesenchymal stem cells. *Aging Cell* 2017;16:183-91.
 97. Kulkarni R, Bajaj M, Ghode S, et al. Intercellular Transfer of Microvesicles from Young Mesenchymal Stromal Cells Rejuvenates Aged Murine Hematopoietic Stem Cells. *Stem Cells* 2018;36:420-33.
 98. Neri S, Borzi RM. Molecular Mechanisms Contributing to Mesenchymal Stromal Cell Aging. *Biomolecules* 2020;10:340.
- (English Language Editor: A. Kassem)

Cite this article as: Huang P, Zhou Y, Li XH, Zhang YN, Cheng HP, Fu JF, Liu W, Yue S, Luo ZQ. N-methyl-D-aspartate receptor blockers attenuate bleomycin-induced pulmonary fibrosis by inhibiting endogenous mesenchymal stem cells senescence. *Ann Transl Med* 2022;10(11):642. doi: 10.21037/atm-22-2507